Highly efficient photon-to-electron conversion with mercurochrome-sensitized nanoporous oxide semiconductor solar cells

Kohjiro Hara[a], Takaro Horiguchi[b], Tohru Kinoshita[b], Kazuhiro Sayama[a], Hideki Sugihara[a], Hironori Arakawa[a,*]

[a]*National Institute of Materials and Chemical Research, 1-1 Higashi, Tsukuba-City, Ibaraki 305-8565, Japan*
[b]*Sumitomo Osaka Cement Co. Ltd., 585 Toyotomi, Hunabashi, Chiba 274-8601, Japan*

Abstract

Dye-sensitized solar cells based on nanoporous oxide semiconductor thin films such as TiO_2, Nb_2O_5, ZnO, SnO_2, and In_2O_3 with mercurochrome as the sensitizer were investigated. Photovoltaic performance of the solar cell depended remarkably on the semiconductor materials. Mercurochrome can convert visible light in the range of 400–600 nm to electrons. A high incident photon-to-current efficiency (IPCE), 69%, was obtained at 510 nm for a mercurochrome-sensitized ZnO solar cell with an I^-/I_3^- redox electrolyte. The solar energy conversion efficiency under AM1.5 (99mWcm^{-2}) reached 2.5% with a short-circuit photocurrent density (J_{sc}) of 7.44mA cm^{-2}, a open-circuit photovoltage (V_{oc}) of 0.52 V, and a fill factor (ff) of 0.64. The J_{sc} for the cell increased with increasing thickness of semiconductor thin films due to increasing amount of dye, while the V_{oc} decreased due to increasing of loss of injected electrons due to recombination and the rate constant for reverse reaction. Dependence of photovoltaic performance of mercurochrome-sensitized solar cells on semiconductor particles, light intensity, and irradiation time were also investigated. High performance of mercurochrome-sensitized ZnO solar cells indicate that the combination of dye and semiconductor is very important for highly efficient dye-sensitized solar cells and mercurochrome is one of the best sensitizers for nanoporous ZnO photoelectrode. In addition, a possibility of organic dye-sensitized oxide semiconductor solar cells has been proposed as well as one using metal complexes. © 2000 Elsevier Science B.V. All rights reserved.

Keywords: Mercurochrome; Nanoporous oxide semiconductor thin film; Dye-sensitization; Electrochemical solar cell; Zinc oxide

* Corresponding author. Fax: + 81-298-54-4750.
E-mail address: khara@nimc.go.jp (H. Arakawa).

1. Introduction

Grätzel and co-workers reported that a dye-sensitized solar cell based on cis-dithiocyanato bis (4,4'-dicarboxy-2,2'-bipyridine) ruthenium (II) (Ru(dcbpy)$_2$(NCS)$_2$) and nanoporous TiO$_2$ thin-film electrodes with an I$^-$/I$_3^-$ redox electrolyte (Grätzel cell) showed a highly efficient solar energy conversion to electricity of 7.1–10% under 1 sun (AM1.5) [1,2]. Since then, many workers have been extensively investigating this dye-sensitization system using various metal complex sensitizers and nanoporous TiO$_2$ electrodes because of its high performance and low cost. Recently, we have reported that a Ru phenanthroline complex (cis-Dithiocyanato bis (4,4'-dicarboxy-2,2'-biphenanthroline) ruthenium (II)) also showed good performance as a sensitizer for dye sensitization with a nanoporous TiO$_2$ thin film and the iodine redox system. The solar energy conversion efficiency under 100 mW cm^{-2} was 6.1% and a high IPCE value, 60% was obtained at 500 nm [3].

In early work of dye sensitization of wide gap semiconductor by Gerischer and co-workers, they used ZnO for the semiconductor electrode and organic dyes as the photosensitizer. For example, 9-phenylxanthene dyes such as rose bengal, fluorescein, rhodamine B, and eosin are known to be good photosensitizers [4,5]. Tsubomura and co-workers studied photosensitization using a porous ZnO electrode and rose bengal as the sensitizer [6]. However, a monochromatic incident photon-to-current efficiency (IPCE) is low such as 15% at 563 nm. In recent work, several studies of dye-sensitized solar cells using organic dyes as sensitizer have also been reported. Cherepy et al. reported a dye-sensitized TiO$_2$ photoelectrochemical cell utilizing flavonoid anthocyanin dyes extracted from blackberries [7]. A solar light to electrical power conversion efficiency, 0.56% with the short-circuit photocurrent densities (J_{sc}) of 1.5–2.2 mA cm^{-2} and the open-circuit photovoltage (V_{oc}) of 0.4–0.5 V was obtained under 1 sun. They also studied the ultrafast excited state dynamics of cyanin dye in solution and adsorbed on TiO$_2$ and ZrO$_2$. Ferrere et al. have studied dye sensitization of nanocrystalline SnO$_2$ electrodes using perylene derivatives [8]. As a result, an overall cell efficiency of 0.89% ($J_{sc} = 3.26$ mA cm^{-2} and $V_{oc} = 0.45$ V) was obtained under 1 sun. Kamat and co-workers have studied dye-sensitization systems, rhodamine 6G/SnO$_2$ and merocyanine 540/TiO$_2$ nanoporous electrodes especially concerning dye aggregation [9,10]. Tennakone and co-workers have used natural pigments, cyanidin and santalin as the photosensitizer for dye-sensitized TiO$_2$ solar cells [11,12]. A 1.8% solar energy conversion efficiency under 80 mW cm^{-2} was obtained for a TiO$_2$/santalin/p-CuI solar cell [12].

We have investigated more than 80 kinds of organic dyes such as 9-phenylxanthene, coumarin, acridine, tetra-phenylmethane, azo, and quinone dyes as the photosensitizer for dye-sensitized nanocrystalline oxide semiconductor solar cells. As a result, eosin yellow (9-phenylxanthene dye) showed a good performance as a sensitizer for TiO$_2$ nanoporous thin-film electrodes [13]. An IPCE of 51% at 533 nm and a solar energy conversion efficiency of 1.3% (AM1.5, 100 mW cm^{-2}) were obtained. Mercurochrome (merbromin) whose structure is presented in Scheme 1, has been used as an antiseptic and a photosensitizer for oxygenation reactions that occur via the singlet oxygen pathway [14]. Recently, we have found that mercurochrome also plays a very good role as a
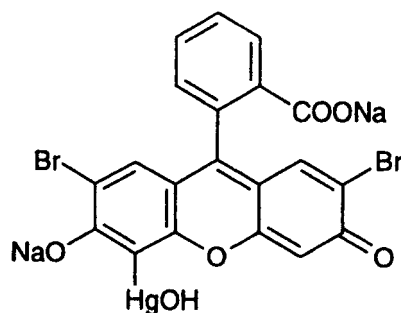
Scheme 1.

photosensitizer for nanoporous oxide semiconductor electrodes [15]. Though Gomes et al. discussed the mechanism of the dye sensitization using a single-crystal ZnO and xanthene dyes containing mercurochrome [16], photovoltaic properties of mercurochrome-sensitized nanoporous oxide semiconductor thinfilm solar cells with an iodine redox electrolyte has never been reported so far. In this work, we have studied mercurochrome as a photosensitizer for a dye-sensitization system based on several nanoporous oxide semiconductor thin-film electrodes such as TiO_2, ZnO, SnO_2, Nb_2O_5, and In_2O_3 for the first time. We have already shown that several kinds of oxide semiconductor materials except for TiO_2, also serve as the photoelectrode for the Grätzel cell using $Ru(dcbpy)_2(NCS)_2$ complex [17]. In this publication, we report the excellent photoelectrochemical properties of dye-sensitized solar cells based on mercurochrome-adsorbed several oxide semiconductor nanocrystalline thin-film electrodes with the iodine redox, and a possibility of organic dyesensitized oxide semiconductor solar cells as well as one using metal complexes.

2. Experimental

2.1. Preparation of semiconductor thin films

2.1.1. Doctor blade method using aqueous paste

Commercial oxide semiconductor powder, Nb_2O_5, ZnO, SnO_2, In_2O_3 (Wako chemical), and TiO_2 (Nippon Aerosil, P25) were used as materials of nanoporous semiconductor electrodes for the doctor blade preparation. The surface areas of these semiconductor powders are shown in Table 1. The aqueous slurry was prepared from 2g of oxide semiconductor powder, distilled water (4 ml), 10 μl of acetylacetone (Wako), and 50 μl of Triton X-100 (Aldrich) as the surfactant. These pastes were deposited on transparent conducting glass supports using a Scotch tape as the spacer with the doctor blade painting method and then calcined at 500℃ for 1 h under air. SnO_2-coated glass (10Ω/sq, transparency 80% Nippon Sheet Glass Co., and 8Ω/sq, transparency 80% Asahi Glass Co.) were used for the transparent conducting glass support. Only TiO_2 thin films were dipped in 0.1 mol dm^{-3} $TiCl_4$ (Wako) aqueous solution for over 18 h at 20℃ and then calcined at 500℃ for l h under air ($TiCl_4$ treatment). The $TiCl_4$ treatment is known to

improve the injection efficiency for dye-sensitized solar cells [2, 13]. Actually, the photocurrent for solar cells increased with the $TiCl_4$ treatment. The thickness of the thin films prepared by the doctor blade method, which depends strongly on the amount of the slurry was 6–40 μm.

2.1.2. Screen printing method using organic paste

Compositions of organic paste of oxide semiconductors for screen printing preparation are the following: TiO_2 (Nippon Aerosil, P25), ethyl cellulose (Kanto) as a binder, and α-terpineol (Kanto) as a solvent for the TiO_2 paste; ZnO nanoparticle (Sumitomo Osaka Cement, #100), polyvinyl acetal (Sekisui Kasei, BM-2), and α-terpineol for the ZnO paste; SnO_2 nanoparticle, polyvinyl acetal, and isophorone (Kanto) for the SnO_2 paste. The In_2O_3 paste was prepared from In_2O_3 nanoparticles, ethyl cellulose as a binder, and α-terpineol. Nanoparticles of SnO_2 and In_2O_3 were prepared from calcination of respective hydroxides precipitated with pH adjustment of $SnCl_4$ (Kanto) and $In(NO_3)_3$ (Kanto) solutions with NH_3. The mixture of these components was dispersed sufficiently with a homogenizer (Janke and Kunkel Ultra-turrax T25) to obtain a homogeneous paste. The paste was printed on a SnO_2-coated conducting glass substrate using screen printing machine (Mitani Electronics Co., MEC 2400) with a suitable screen mesh and then calcined for 1 h at 420℃ for ZnO and at 500℃ for other oxides. The thickness and area of thin films can be easily controlled by selection of paste composition, screen mesh size, and repetition of printing.

2.2. Dye adsorption on oxide semiconductor thin films

A 0.5 mmol dm^{-3} ethanolic solution of mercurochrome was prepared from mercurochrome (Aldrich) and dehydrated ethanol (Wako) without further purifications. Semiconductor thin films were immersed into this solution and then refluxed at 80℃ for 1 h to fix the dye on the surface of semiconductor electrodes. Before dye adsorption, semiconductor thin films were calcined at 500℃ for 1 h to eliminate water adsorbed on the semiconductor surface. Dye adsorption procedure can be also conducted at 20℃ for over 18 h instead of reflux condition. After dye adsorption, the color of the thin films changed to a deep red.

2.3. Characterization

Absorption spectra of mercurochrome in ethanol and adsorbed on oxide semiconductor thin films were measured using Shimadzu MPS-2000 and UV-3101PC with transmission and diffuse reflectance mode. Amount of dye adsorbed on semiconductor was evaluated from the absorbance in the solution after dye was desorbed from semiconductor thin films by dipping in 1.0 mmol dm^{-3} NaOH ethanol/H_2O (50:50) solution. Emission spectra of mercurochrome were measured with Hitachi F-4500. IR absorption spectra were measured using Perkin-Elmer System 2000 FT-IR with transmission and diffuse reflectance mode. Thickness of the oxide semiconductor thin films was measured using an Alpha-Step 300 profiler (Tencor Instruments). SEM measurements of

thin films was conducted with Hitachi S-800. Oxidation potential of mercurochrome in ethanol solution was estimated using a normal three-compartment cell with a carbon and an Au working electrode, a Pt counterelectrode, and an Ag/AgCl reference electrode in saturated KCl solution. Measurement was conducted using an electrochemical measurement system, BAS100B and a potentio/galvanostat (Hokuto Denko Ltd., HA-501), an arbitrary function generator (Hokuto, HB-105), and an XY recorder (Riken Denshi co. Ltd., F-5C).

2.4. Photoelectrochemical measurements

A sandwich-type two-electrode electrochemical cell for photovoltaic measurement consists of a dye-adsorbed semiconductor electrode, a counterelectrode, a spacer, and an organic electrolyte. The counterelectrode was a Pt sputtered on a transparent conducting glass using an ion coater (Eiko engineering, IB-5). The spacer was polyethylene films (thickness 30 and 120 μm). Electrolyte was a 0.5 mol dm^{-3} Pr$_4$NI-0.05 mol dm^{-3} I$_2$/ethylene carbonate-acetonitrile (60:40) solution and a 0.3 mol dm^{-3} LiI-0.03 mol dm^{-3} I$_2$/acetonitrile solution prepared from reagent grade chemicals: Pr$_4$NI (Tokyo Kasei), I$_2$, LiI, ethylene carbonate, acetonitrile (Wako). Apparent surface areas of dye-adsorbed semiconductor electrodes were 0.09 cm^2 (0.03 × 0.03 cm), 0.5 cm^2 (0.5 × 1.0 cm), and 1.0 cm^2 (1.0 × 1.0 cm).

Photoelectrochemical performance of the solar cells was measured with a potentio/galvanostat (Nikko Keisoku, NPGS-2501), a digital multimeter (Escort, EDM-2116), and an XY recorder (Graphtec, WX1100). The light source was a 500 W Xe lamp with a < 420 nm cut-off filter and an ND 25 filter. In addition, an AM1.5 solar-simulated light source system (Wacom, WXS-80C-3) was also used. A 500 W halogen lamp, a monochrometer (Jasco, CT-10), a scanning controller (Jasco, SMD-25C), and a multimeter (Keithley, 2000) were used for the IPCE measurements of the solar cells. Light intensities of monochromatic and solar-simulated light were estimated with an optical power meter (Advantest, TQ8210) and a thermopile (The Eppley Lab., Inc., Newort, R.I.), respectively.

3. Results and discussion

3.1. Characterization

Fig. 1 shows absorption spectra of the mercurochrome in ethanol and adsorbed on a TiO$_2$ nanoporous thin film. The absorption peak of mercurochrome in ethanol was 517 nm and molar absorption coefficient at 517 nm was 7.4×10^7 mol^{-1} cm^{-2}. The shoulder which is attributed to the absorption of a dimer is observed at 480 nm [18]. Such absorption behaviors agree with those of 9-phenylxanthene dyes such as eosin yellow [19]. For the absorption spectrum of mercurochrome adsorbed on a TiO$_2$ substrate, absorption intensity due to the dimer increased compared to that in ethanol, indicating that the dimer of mercurochrome is formed on the TiO$_2$ surface. The dimer of 9-
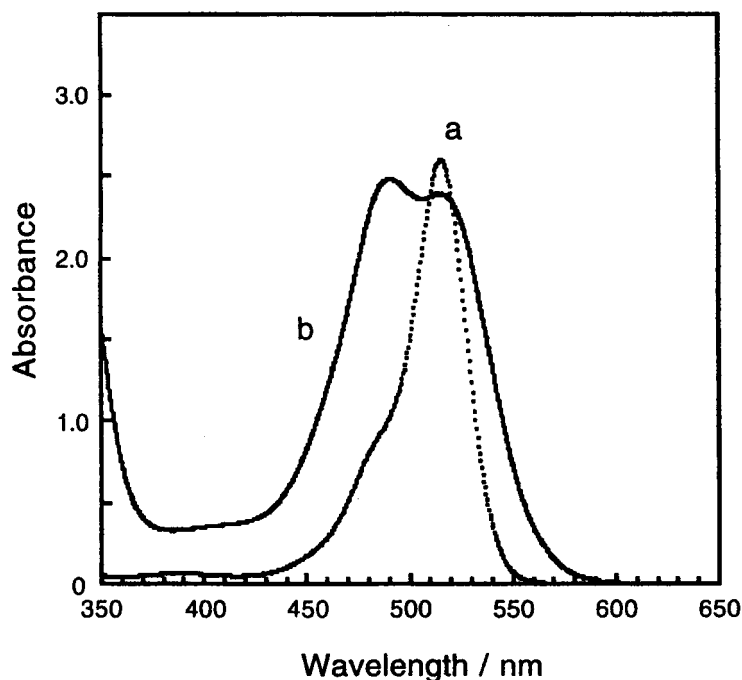
Fig. 1. Absorption spectra of mercurochrome: (a) free dye in ethanol solution and (b) adsorbed on a TiO$_2$ nanoporous thin film.

phenylxanthene dyes is known to be formed even in solutions at high concentrations. The absorption spectrum of mercurochrome adsorbed on TiO$_2$ is more broad compared to that in ethanol solution. The onset of absorption is shifted from 560 to 590 nm, as shown in Fig. 1. This can be explained by a change in the energy levels of HOMO and LUMO of mercurochrome compared to those in solution, due to the interaction between mercurochrome molecules and the TiO$_2$ substrate.

Fig. 2 shows emission spectrum for mercurochrome in ethanol. Emission spectra in ethanol with a colloidal SiO$_2$ and TiO$_2$ are also shown in this figure. The emission peak was observed at 540 nm. Generally, 9-phenylxanthene dyes such as fluorescein show a small storks shift [20]. The 0–0 transition energy estimated from the cross section between the absorption and the emission spectra is 2.35 eV (535 nm). The emission intensity decreases drastically in the presence of colloidal TiO$_2$, as shown in Fig. 2, indicating that electron injection from mercurochrome into the conduction band of TiO$_2$ occurs. A small decrease in the emission intensity was also observed in the solution with SiO$_2$ particle, while electron injection from mercurochrome into SiO$_2$ is considered to hardly occur. Kamat et al. reported that the emission of rhodamine 6G in solution decreased with addition of colloidal SiO$_2$ [9]. They explained this phenomenon by static quenching, i.e. electron transfer between dyes due to dimer formation on the SiO$_2$ surface.

IR absorption spectra of mercurochrome in diffuse reflectance mode are shown in Fig. 3. The absorption peak at 1540 cm^{-1} for mercurochrome is attributed to O–C–O asymmetric stretching band of carboxyl group (spectrum a). The peaks at 1300–1400
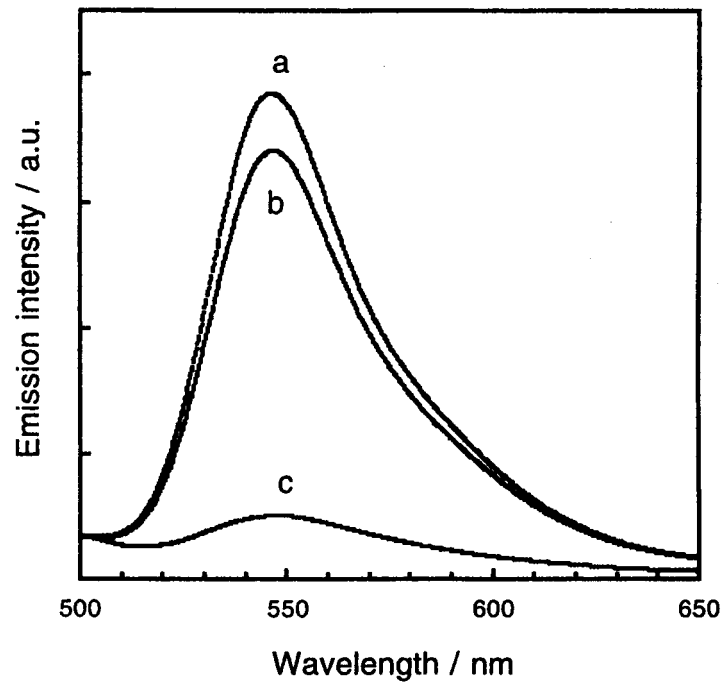
Fig. 2. Emission spectra of mercurochrome in ethanol solution: (a) without colloidal particles, (b) with colloidal SiO_2, and (c) with colloidal TiO_2.
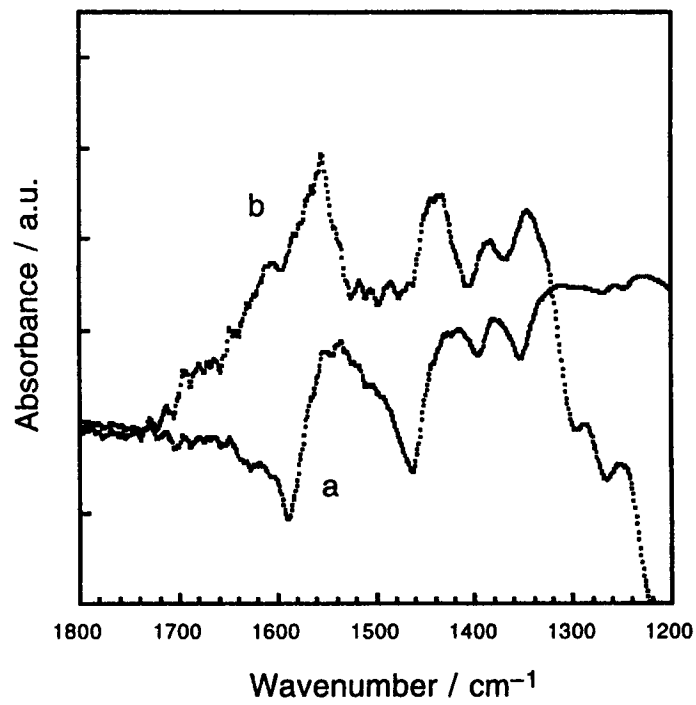
Fig. 3. IR absorption spectra of mercurochrome in diffuse reflectance mode: (a) free mercurochrome and (b) mercurochrome adsorbed on TiO_2.

cm^{-1} are due to O–C–O symmetric stretching band. The absorption of O–C–O asymmetric stretching is observed at 1560 cm^{-1} for mercurochrome adsorbed on TiO_2, as shown in Fig. 3 (spectrum b). O–C–O stretching band around near 1700 cm^{-1} attributed to the ester bonding is not observed. This indicates that mercurochrome molecules are adsorbed on TiO_2 substrate with carboxylate COO^- linkage. A similar absorption spectrum was obtained for mercurochrome adsorbed on ZnO, indicating that there is no effect of the semiconductor on adsorption linkage. All absorption peaks of mercurochrome adsorbed on TiO_2 are shifted about 20 cm^{-1} to large wave numbers compared to the peaks of free dye, as shown in Fig. 3. This shift is due to the interaction between dye molecule and TiO_2. It has been reported that Ru complexes such as $Ru(dcbpy)_2(NCS)_2$ are adsorbed on the TiO_2 surface with esterlike bonding [18,21,22]. The strong peak at 1600 cm^{-1} showing the presence of carboxylate linkage was also observed for $Ru(dcbpy)_2(NCS)_2$ complex adsorbed on ZnO, indicating that adsorption mode of $Ru(dcbpy)_2(NCS)_2$ depends upon the kind of semiconductor materials [17].

Fig. 4 presents SEM photographs of nanoporous oxide semiconductor electrodes. The porous structure of the materials is clearly observed in these photographs. TiO_2 particles (P25) have 30–50 nm diameter which is known to be larger than that for colloidal TiO_2 prepared from the hydrolysis of Ti-alkoxides. SnO_2 particle has a small diameter of 15–25 nm, as shown in Fig. 4b. A commercial ZnO-A purchased from Wako, has a large size, 100–400 nm, and a high crystallinity, resulting in the only small surface area (Fig. 4c). Particle size of the other ZnO-B supplied from Sumitomo Osaka Cement, sintered at 420℃ is 20–40 nm (Fig. 4c). At higher sintering temperature, crystallinity and particle size of ZnO will increase because ZnO particle grows easily at high temperature. In_2O_3 nanoparticles have a small particle size of 15–25 nm as well as SnO_2 particle Transparent thin films were obtained using these ZnO-B, SnO_2, and In_2O_3 nanoparticles while a TiO_2 film made from P25 particle was translucent and ZnO-A film is quite white. The band gap of these nanoparticle semiconductors estimated from the onset of the absorption spectra was 3.2 eV for ZnO, 3.6 eV for SnO_2, and 2.9 eV for In_2O_3.

3.2. Photovoltaic properties for mercurochrome-sensitized solar cells

Table 1 shows the photovoltaic properties of mercurochrome-sensitized oxide semiconductor solar cells with an I^-/I_3^- redox under light intensities of 83 and 100 mW cm^{-2} (AM1.5). Firstly, we describe the photovoltaic properties of mercurochrome-sensitized solar cells based on semiconductor photoelectrodes prepared from commercial semiconductor powder by the doctor blade technique. Mercurochrome can function as an efficient sensitizer for dye-sensitized oxide semiconductor solar cells and photovoltaic properties depend remarkably upon the semiconductor materials, as shown in this table. For Bi_2O_3 and Nb_2O_5, photocurrent was hardly obtained (0.014 mA cm^{-2} for Bi_2O_3 and 0.041 mA cm^{-2} for Nb_2O_5). The V_{oc} was 0.31 V for Bi_2O_3 and 0.54 V for Nb_2O_5. Intermediate performance was obtained for ZnO and SnO_2 electrodes. A large J_{sc}, 2.38 mA cm^{-2}, was observed for an In_2O_3 electrode, while the V_{oc} of 0.39 V is lower than those for other semiconductor electrodes. The total photon-to-current energy conversion effi-
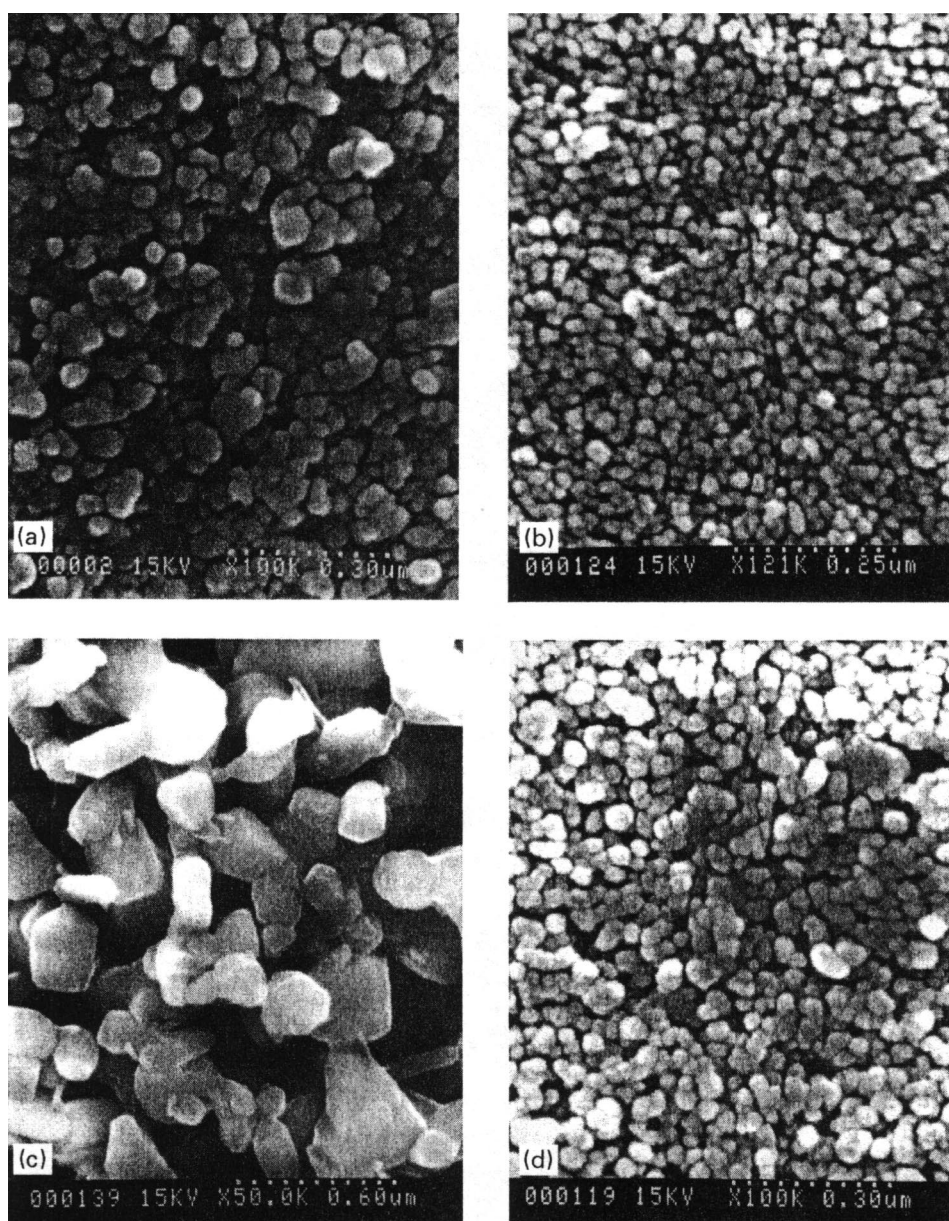
Fig. 4. SEM photographs of nanoporous oxide semiconductor thin films: (a) TiO_2 (P25), (b) SnO_2, (c) ZnO (Wako), and (d) ZnO (Sumitomo Osaka Cement).

ciency, η, for the TiO_2 electrode is 1.44% ($J_{sc} = 2.10$ mA cm^{-2}, $V_{oc} = 0.78$ V, and ff = 0.73).

The photovoltaic performance of mercurochrome-sensitized solar cells based on nanoparticle ZnO, SnO_2, and In_2O_3 thin-film photoelectrodes prepared from organic paste by screen printing is also shown in Table 1. The η under AM1.5 (100 mW cm^{-2}) reached 1.44% with a J_{sc} of 4.04 mA cm^{-2} for a nanoparticle ZnO-A (SOC) electrode, while the η was 0.75% for a large particle of ZnO-B (Wako) with a J_{sc} of 2.17 mA cm^{-2}.

Table 1
Photovoltaic performance of mercurochrome-sensitized oxide semiconductor solar cells[a]

Semiconductor	Particle size (nm)	Surface area ($m^2\,g^{-1}$)	Electrode area (cm^2)	Thickness (μm)	Dye amount ($10^{-8}\,mol\,cm^{-2}$)	J_{sc} ($mA\,cm^{-2}$)	V_{oc} (V)	Fill factor	η (%)
Bi_2O_3 (Wako)[b]	—	—	1.0	—	—	0.014	0.31	0.31	0.002
Nb_2O_5 (Wako)[b]	100	—	1.0	19	—	0.041	0.54	—	—
SnO_2 (Wako)[b]	60	5	1.0	10	—	0.88	0.66	0.65	0.45
In_2O_3 (Wako)[b]	100–500	8	1.0	35	—	2.38	0.39	0.29	0.32
ZnO (Wako)[b]	100–400	6	1.0	14	—	1.01	0.63	0.63	0.48
TiO_2 (P25)[b]	30–50	49	1.0	10	11	2.10	0.78	0.73	1.44
ZrO_2 (SOC)[c]	10–15	—	0.25	6	—	0.004	0.14	—	—
SnO_2 (SOC)[c]	15–25	94	0.25	5	7.5	1.95	0.58	0.56	0.64
In_2O_3 (SOC)[c]	15–25	56	0.25	7	6.2	5.35	0.24	0.29	0.38
ZnO (SOC)[c]	20–40	43	0.25	8	6.2	4.04	0.62	0.57	1.44
ZnO (SOC)[c]	20–40	43	0.09	36	25	7.44	0.52	0.64	2.52
ZnO (Wako)[c]	100–400	6	0.25	5	0.7	2.17	0.60	0.57	0.75

[a] Electrolyte: $0.3\,mol\,dm^{-3}\,Pr_4NI + 0.03\,mol\,dm^{-3}\,I_2$/ethylene carbonate–acetonitrile (60:40).
[b] Semiconductor thin films were prepared with doctor blade method from aqueous colloidal solutions. The light source is a 500 W Xe lamp with a > 420 nm cut filter and ND25 filter ($83\,mW\,cm^{-2}$).
[c] Semiconductor thin films were prepared with screen printing from organic paste. The light source is an AM1.5 solar simulator ($100\,mW\,cm^{-2}$).

Amounts of mercurochrome adsorbed on two of the ZnO thin films were 6.2×10^{-8} mol cm^{-2} for ZnO-A (thickness 7.9 μm) and 0.7×10^{-8} mol cm^{-2} for ZnO-B (thickness 5.0 μm). Six times the amount of mercurochrome for 1 μm thickness is adsorbed on the ZnO-A thin-film compared to that for ZnO-B. Light harvesting efficiency (LHE) is represented by the following equation [2]:

$$\text{LHE} = 1 - T = 1 - 10^{-\text{abs}} = 1 - 10^{\Gamma\sigma} , \tag{1}$$

where T is the transmittance, abs is the absorbance, Γ is the amount of dye for 1 cm^2, σ is the molar absorption coefficient (absorption cross section, mol^{-1} cm^{-2}). According to σ for mercurochrome, 7.4×10^7 mol^{-1} cm^2, and Eq. (1), the LHE is 70% for ZnO-B thin-film and 99% for ZnO-A, respectively. A larger J_{sc} for the ZnO-A nanoparticle thin-film compared to ZnO-B is explained by an increase in LHE due to a large amount of mercurochrome adsorbed on large surface area of small ZnO nanoparticles. However, the J_{sc} for ZnO-A is approximately 2 times that for ZnO-B, as shown in Table 1, while six times of mercurochrome is adsorbed, suggesting that all of dye molecules absorbing photon do not participate in the electron injection process. The η for the ZnO-A electrode increases to 2.52% with increasing thickness (36 μm) and dye amount (25×10^{-8} mol cm^{-2}). In addition, photoelectrodes using SnO$_2$ and In$_2$O$_3$ nanoparticles (15–25 nm) also show good photovoltaic performance, as shown in Table 1 (the J_{sc} value of 5.35 mA cm^{-2} for In$_2$O$_3$).

It was reported that the amount of Ru(dcbpy)$_2$(NCS)$_2$ complex adsorbed on a TiO$_2$ nanoporous thin-film (thickness 10 μm) was 1.2×10^{-7} mol cm^{-2} [2]. The amount of eosin yellow adsorbed on a TiO$_2$ film (7 μm) is 4.5×10^{-9} mol cm^{-2} [13]. As shown in Table 1, the amounts of mercurochrome adsorbed on nanoporous semiconductor thin films, 11×10^{-8} mol cm^{-2} for 10 μm TiO$_2$, 6.2×10^{-8} mol cm^{-2} for 8 μm ZnO, and 25×10^{-8} mol cm^{-2} for 36 μm ZnO, are equal to that of Ru(dcbpy)$_2$(NCS)$_2$ complex. The coverage of mercurochrome molecules on the TiO$_2$ surface can be evaluated from the dye amount of 11×10^{-8} mol cm^{-2} for a TiO$_2$ thickness of 10 μm, the area of mercurochrome molecule 0.3 nm^2, a porosity of 50% [23], a surface area of TiO$_2$ of 50 m^2 g^{-1}, and a density of 4 g cm^{-3}. Approximately, 20% of the TiO$_2$ surface is covered with mercurochrome molecules. The photovoltaic property of solar cell can be improved with increasing the coverage of mercurochrome due to prevention of the back electron transfer reaction which leads to a decrease in V_{oc} [2].

The relationship between V_{oc} for mercurochrome-sensitized solar cells and the potential of the conduction band of semiconductors [23–26] is shown in Fig. 5. V_{oc} increases with more negative potential of the conduction band. For TiO$_2$, ZnO, and Nb$_2$O$_5$ which have more negative potentials of the conduction band, high photovoltage can be obtained due to large energy gap with the iodine redox potential, while Bi$_2$O$_3$ and In$_2$O$_3$ whose potential of the conduction band are more positive, produce only low photovoltage. A large photocurrent observed for In$_2$O$_2$ electrode is considered to be due to a large driving force for electron injection with a large energy gap between the conduction band and LUMO of mercurochrome. A quite small photocurrent for ZrO$_2$, as shown in Table 1, is due to more negative potential of the conduction band compared to those for other
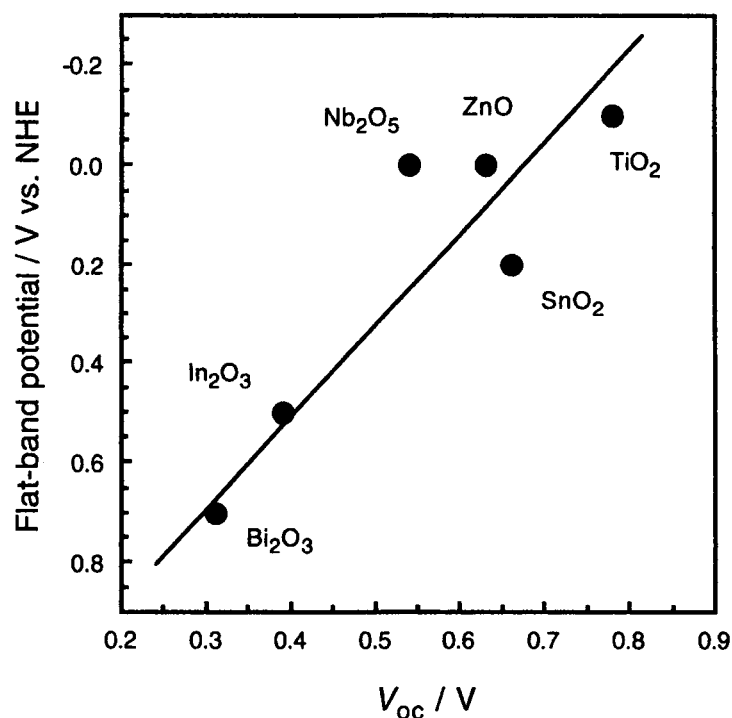
Fig. 5. Relationship between the V_{oc} for mercurochrome-sensitized solar cells and the potential of the conduction band of semiconductors.

semiconductors, suppressing electron injection from LUMO of mercurochrome. A similar relationship between V_{oc} for dye-sensitized solar cell and the potential of conduction band of semiconductors was obtained in the $Ru(dcbpy)_2(NCS)_2$-sensitized solar cell [17].

In addition to the energy potential of the conduction band, linkage between semiconductor and dye molecule is very important for effective electron injection. Goodenough et al. reported that the conduction band of semiconductors being d-orbitals may be one of the most important factors for increasing electron injection efficiency for dyes having an anchor group as an electron pathway [27]. The conduction bands of TiO_2, Nb_2O_5, and ZrO_2 consist of d-orbitals, while those of ZnO, SnO_2, and In_2O_3 are s-orbitals. However, it is suggested that mercurochrome molecules are adsorbed on both TiO_2 and ZnO surfaces with the chelating absorption by a carboxylate COO^- linkage, as mentioned above. In addition, ZnO and In_2O_3 electrodes show good performance of photon-to-current energy conversion similar to TiO_2, as shown in Table 1. These results indicate that electron injection from mercurochrome into the semiconductors conduction band occurs effectively with carboxylate coordination, being independent of the kind of semiconductor materials and suggest that other physical properties of semiconductor such as energy level of conduction band and conductivity are important for good performance of solar cell based on mercurochrome-sensitized semiconductor photoelectrodes. In addition, it is also suggested that the electron injection from xanthene dyes such as
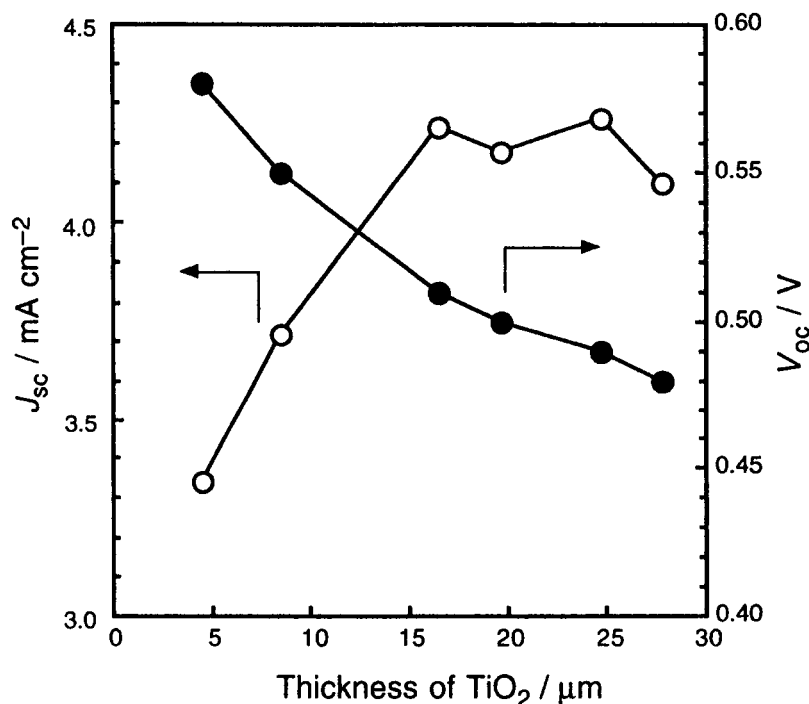
Fig. 6. Relationship between the photovoltaic properties for a mercurochrome-sensitized TiO_2 solar cell and the thickness of the TiO_2 thin-film electrode: (○) J_{sc} and (●) V_{oc}. Light source: a 500 W Xe lamp with $a < 420$ nm cut-off filter and an ND25 filter.

mercurochrome is not only bond-through pass, but also space-through pass while that for $Ru(dcbpy)_2(NCS)_2$ is considered to be bond-through pass.

3.3. Effect of thickness of thin-film on photovoltaic property

Fig. 6 shows the relationship between photovoltaic performance (J_{sc} and V_{oc}) for a mercurochrome-sensitized TiO_2 solar cell and thickness of the TiO_2 thin-film electrode. The electrolyte is a 0.3 mol dm^{-3} LiI-0.03 mol dm^{-3} I_2/acetonitrile solution and the apparent surface area of the TiO_2 electrode was 0.5 cm^2 (0.5 cm × 1.0 cm). The J_{sc} increases with increasing thickness of the TiO_2 film (J_{sc} = 2.3 mA cm^{-2} for 4.5 μm and J_{sc} = 3.1 mA cm^{-2} for 25 μm thin film). This is due to an increase in the amount of adsorbed dye with increasing TiO_2 thickness. On the other hand, the V_{oc} decreases from 0.71 to 0.58 V with increasing thickness from 4.5 to 28 μm. An increasing thickness would lead to increasing loss of injected electrons due to recombination in the electron transfer process in TiO_2 nanoparticles and increasing series resistance of the cell, resulting in a decrease in photovoltage and ff. In addition, it is known that V_{oc} for a dye-sensitized solar cell decreases with enhancement of the back electron transfer reaction concerning reduction of I_3^- to I^- with injected electrons [2]. The decrease in V_{oc} with increasing thickness is also explained by enhancement of the back reaction with increasing non-dye-adsorbed TiO_2 sites.
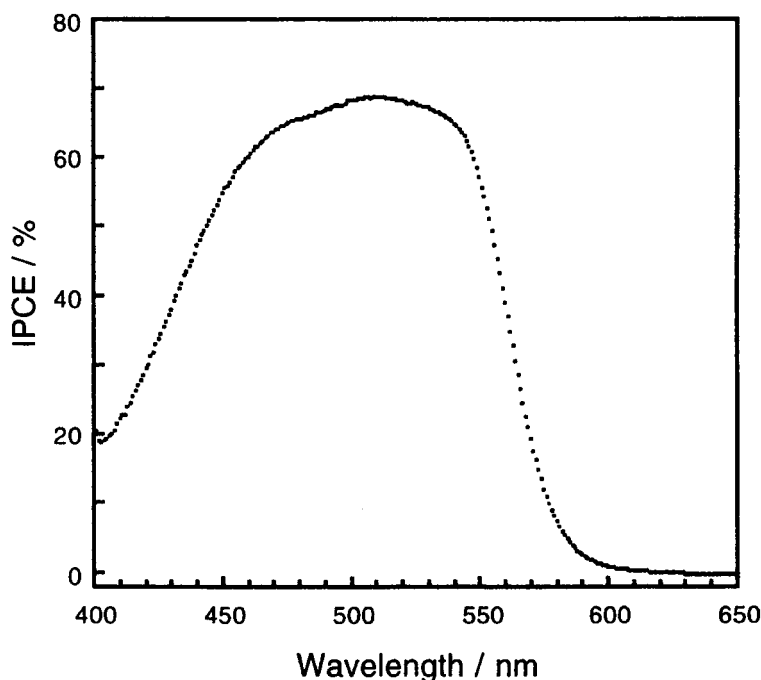
Fig. 7. An action spectrum of IPCE for the solar cell based on mercurochrome-sensitized ZnO thin-film electrode (20 μm thickness and 0.5 cm^2) with an I$^-$/I$_3^-$ redox electrolyte.

3.4. Photon-to-electron energy conversion efficiency

Fig. 7 shows the action spectrum of IPCEs for the mercurochrome-sensitized nanoporous ZnO solar cell (20 μm thickness and 0.5 cm^2) with an I$^-$/I$_3^-$ redox electrolyte. This solar cell can efficiently convert visible light in the region from 400 to 600 nm to photocurrent, as shown in this figure. The maximum IPCE reached 69% at 510nm. IPCE is represented by the following equation:

$$IPCE = LHE \times \phi_{inj} \times \eta_c, \tag{2}$$

where LHE is the light harvesting efficiency, ϕ_{inj} is the electron injection efficiency and η_c is the electron collecting efficiency at back contact. The LHE for mercurochrome reaches 99%, as described above. Highly efficient IPCEs indicate that electron transfer process from excited mercurochrome to the conduction band of semiconductors occurs effectively. In addition, electron transfer from I$^-$ ion to oxidized mercurochrome is also an effective process. It was reported that the IPCE for dye-sensitized TiO$_2$ solar cells using Ru(dcbpy)$_2$(NCS)$_2$ complex reached 85–90% in the region of 510–570 nm [2,23,25]. On the other hand, a monochromatic IPCE for Ru(dcbpy)$_2$(NCS)$_2$ complex adsorbed on a ZnO electrode (7 μm thickness) was 58% at 540 nm which is lower than that of Ru(dcbpy)$_2$(NCS)$_2$/TiO$_2$ system [28]. An IPCE of 8.5% at 550 nm for a ZnO photoelectrode sensitized with rose bengal was also reported [29]. Note that the IPCE performance of mercurochrome as a sensitizer for a ZnO electrode exceeds those of other dyes significantly.
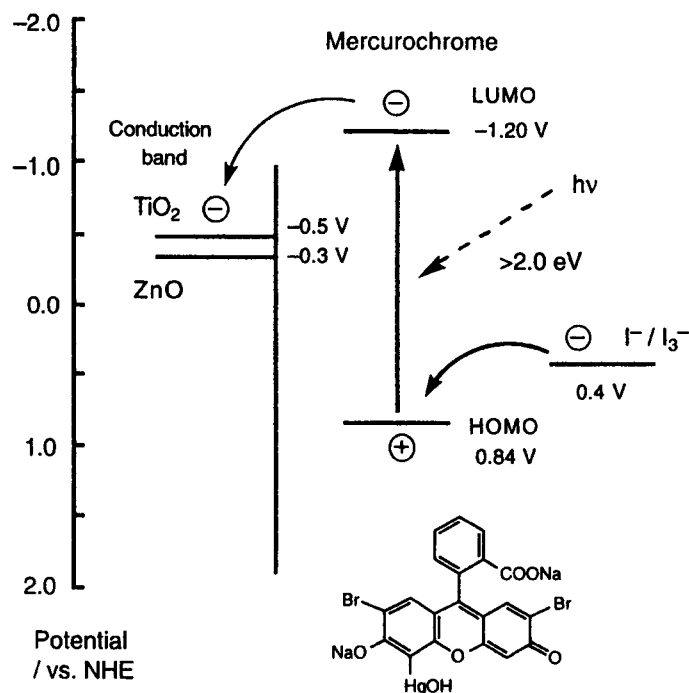
Fig. 8. Energy diagram of mercurochrome-sensitized TiO_2 and ZnO solar cells with an I^-/I_3^- redox electrolyte.

The action spectrum of IPCEs for mercurochrome/ZnO solar cell is relatively broad compared to the absorption spectrum of mercurochrome in ethanol (Fig. 1). The broadening of the action spectrum of IPCE leading to good photoresponse in the visible light can be explained by two factors. (a) Large amount of dye: a large amount of mercurochrome (i.e. 11×10^{-8} mol cm^{-2}, as shown in Table 1) was adsorbed on the semiconductor substrates. Under this condition, saturation of LHE (1-T) especially occurs in 450–550 nm, according to Eq. (1). So a relatively broad shape and plateau are observed in the IPCE spectrum. (2) Change in the energy gap of dye: the onset of the action spectrum of IPCE indicating the energy gap between HOMO and LUMO of mercurochrome is approximately estimated as 2.0 eV (610 nm). On the other hand, the 0–0 energy gap of mercurochrome in ethanol solution, estimated from the intersection between the emission spectrum and the absorption spectrum, is 2.35 eV, as shown above. This energy difference suggests the presence of an interaction between mercurochrome molecules and semiconductor substrates and each dye including the formation of dimer and/or aggregate. These interaction lead to change in the energy levels of HOMO and LUMO of mercurochrome adsorbed on the semiconductor surface, resulting in the broadening of the action spectrum of IPCE. The action spectrum of IPCE for the $Ru(dcbpy)_2(NCS)_2/TiO_2$ solar cell is also relatively broad compared to the absorption spectrum of dye in solution [2,23,25].

Fig. 8 shows the energy diagram of the mercurochrome-sensitized oxide semiconductor solar cells where the conduction bands of TiO_2 and ZnO are –0.5 V vs. NHE [23,25]
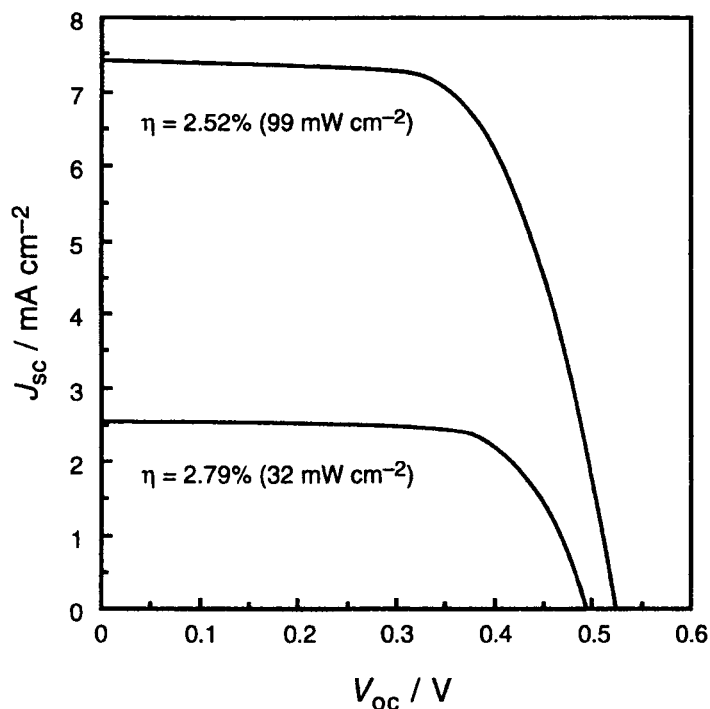
Fig. 9. Photocurrent-voltage curves for a mercurochrome/ZnO solar cell with an I^-/I_3^- redox electrolyte: the ZnO electrode, 36 μm thickness and 0.09 cm^2.

and –0.3 V vs. NHE [30], respectively, and the oxidation potential of I^- ion is 0.4 V vs. NHE [23,25]. The oxidation potential of mercurochrome was measured in an ethanolic solution. An irreversible oxidation peak was observed at 0.62 V vs. Ag/AgCl (0.84 V vs. NHE). The standard oxidation potential for $RuL_2(X)_2(X = Cl^-, Br^-, I^-, CN^-,$ and NCS^-) was 0.85 V vs. SCE (1.05 V vs. NHE) in acetonitrile [2] and that for eosin yellow was 0.84 V vs. SCE (1.04 V vs. NHE) in water and 0.91 V vs. SCE (1.1 V vs. NHE) in ethanol [31]. The oxidation potential for mercurochrome is more negative than those for $RuL_2(NCS)_2$ complexes and eosin yellow.

The photocurrent-voltage curves for a mercurochrome/ZnO solar cell are shown in Fig. 9. The total solar energy conversion efficiency η under AM1.5 (99 mW cm^{-2}) reached 2.5% (J_{sc} = 7.44 mA cm^{-2}, V_{oc} = 0.52 V, and ff = 0.64, as shown in Table 1). The value of η increases to 2.7% on decreasing the light intensity to 39 mW cm^{-2} (J_{sc} = 3.11 mA cm^{-2}, V_{oc} = 0.49 V, and ff= 0.70). The value of η for a Ru(dcbpy)$_2$(NCS)$_2$-sensitized ZnO solar cell was 0.4% at 119 mW cm^{-2} for 0.7 μm thickness of ZnO [32] and 2% at 56 mA cm^{-2} for 30 μm thickness [28]. Note that the performance of a mercurochrome-sensitized nanocrystalline ZnO thin-film solar cell exceeds that of Ru(dcbpy)$_2$(NCS)$_2$/ZnO system, while Ru(dcbpy)$_2$(NCS)$_2$ complex can absorb visible light from 600 to 800 nm where mercurochrome cannot absorb and convert to photocurrent. This suggests that the combination of dye and semiconductor is very important for highly efficient dye-sensitization systems and mercurochrome is one of the best sensitizers for nanoporous ZnO photoelectrode.
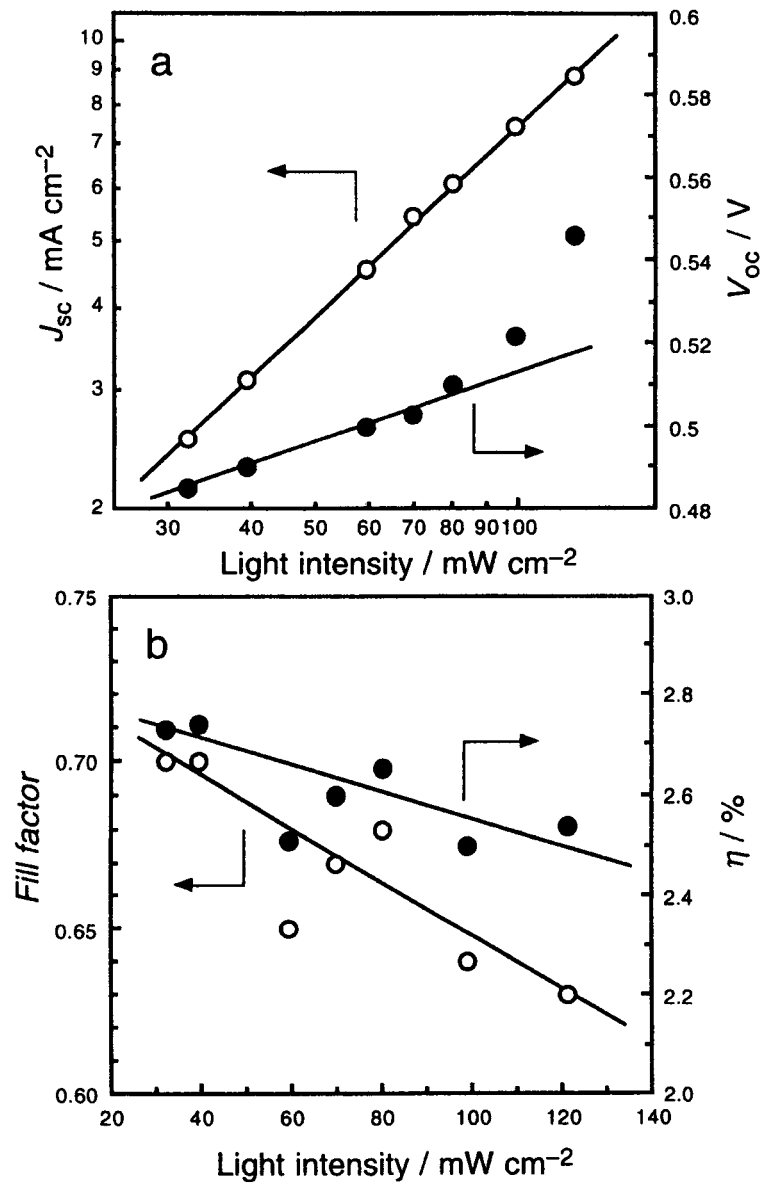
Fig. 10. Dependencies of the photovoltaic property for a mercurochrome-sensitized ZnO solar cell (thickness 36 μm and apparent surface area 0.09 cm²) on the incident light intensity: (a) J_{sc} and V_{oc}, and (b) fill factor and η.

3.5. Light intensity dependence

Fig. 10 shows the dependencies of J_{sc}, V_{oc}, ff, and η for a mercurochrome-sensitized ZnO solar cell (thickness 36 μm and the apparent surface area 0.09 cm²) on the incident light intensity. J_{sc} is proportional to light intensity, indicating no mass transport limitations. Also, the slope of the logarithmic plot of J_{sc} versus intensity is 0.94 which is close to unity, indicating that the photogeneration of charge carriers is a monophotonic pro-
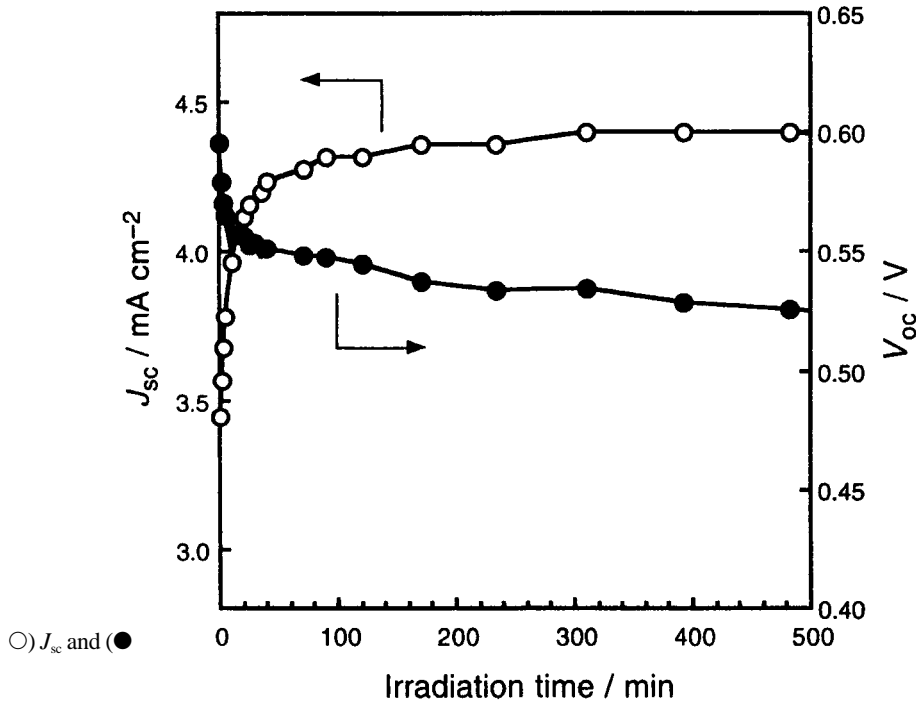
Fig. 11. Irradiation time dependencies of J_{sc} and V_{oc} for a mercurochrome-sensitized ZnO solar cell under visible light irradiation: (○) J_{sc} and (●) V_{oc}, Light source is an AM1.5 solar simulator with $a < 420$ nm cut-off filter (85 mW cm^{-2}).

cess V_{oc} also increases with increasing light intensity. The relationship between V_{oc} and J_{sc} is expressed as follows [33,34]:

$$V_{oc} = \frac{nkT}{q} \ln\left(\frac{J_{sc}}{J_0} + 1\right),$$

(3)

where n is the diode ideality factor, k is the Boltzmann constant, q is the electric charge, and J_0 is the reverse saturation current density. According to Eq. (3), V_{oc} is proportional to the log of light intensity because J_{sc} is proportional to the light intensity. This relationship is observed in Fig. 10a, while deviation is observed at over 70 mW cm^{-2}, suggesting the change of n and/or T with increasing light intensity.

Fill factor for solar cell decreases with increasing incident light intensity (Fig. 10b). This can be explained by an increase in the series resistance of the cell due to an increase in the photocurrent. A decreasing leads to a decreasing η while J_{sc} and V_{oc} increase with increasing light intensity.

3.6. The stability of J_{sc} and V_{oc} for a mercurochrome-sensitized ZnO solar cell

Irradiation time dependencies of J_{sc} and V_{oc} for a mercurochrome-sensitized ZnO solar cell are shown in Fig. 11. Measurement was conducted using an open-cell and the

light intensity was 85 mW cm^{-2} using an AM1.5 solar simulator with $a < 420$ nm cut-off filter. For 15 min from the beginning of irradiation, the J_{sc} increases with increasing time while the V_{oc} decreases and after 15 min, J_{sc} and V_{oc} are constant, as shown in Fig. 11. These changes of J_{sc} and V_{oc} in the initial stage is considered to be due to diffusion of I$^-$ ion into the nanoporous semiconductor film and of I$_3^-$ into the surface of the Pt counter electrode. No degradation of J_{sc} and V_{oc} was observed for 24 h of irradiation. Grätzel et al. showed the photovoltaic stability of sealed dye-sensitized solar cell using Ru(dcbpy)$_2$(NCS)$_2$ complex [35]. The measurement was carried out under visible light irradiation (< 395 nm cut off, 100 mW cm^{-2}). As a result, the photovoltaic performance was stable for more than 7000 h and the turnover number per dye molecule reached 10^7. No degradation of sensitizer was observed after the irradiation, indicating the stable operation of the dye in the solar cell system. In our study, the turnover number for a mercurochrome-sensitized solar cell reached more than 18000 even under the open-cell condition, indicating a sufficient stability of mercurochrome, one of the organic dyes, which is known to be unstable compared to metal complexes, in this system under irradiation. If evaporation of the solvent of the electrolyte can be prevented by the sealing technique, a stability of the cell performance could be achieved for a longer term.

4. Conclusions

We have investigated the photovoltaic performance of dye-sensitized solar cells based on mercurochrome as a photosensitizer and nanoporous oxide semiconductor thin-film electrodes such as TiO$_2$, Nb$_2$O$_5$, ZnO, SnO$_2$, and In$_2$O$_3$ prepared by the doctor blade technique and screen printing. Mercurochrome adsorbed on semiconductor surface can absorb visible light in the range of 400–600 nm. IR absorption spectra suggested that mercurochrome molecules are adsorbed on semiconductor surface with carboxylate linkage while Ru complexes such as Ru(dcbpy)$_2$(NCS)$_2$ are considered to be adsorbed by ester-like bonding.

Good cell performance was especially obtained for TiO$_2$, ZnO, SnO$_2$, and In$_2$O$_3$ solar cells. A high incident photon-to-current efficiency (IPCE), 69%, was obtained at 510 nm for a mercurochrome-sensitized ZnO solar cell with an I$^-$/I$_3^-$ redox electrolyte. The solar energy conversion efficiency, η, under AM1.5 (99 mW cm^{-2}) reached 2.5% with a J_{sc} value of 7.44 mA cm^{-2}, a V_{oc} value of 0.52 V, and an ff value of 0.64. Highly efficient photo-to-electron conversion is considered to be due to a large amount of adsorbed mercurochrome on semiconductor nanoparticles leading to high light harvesting efficiency, and broadening of absorption spectra of dye on semiconductor surface with dye-dye and/or dye-semiconductor interactions.

We also investigated the dependence of photovoltaic performance of mercurochrome-sensitized solar cells on semiconductor particles, light intensity, irradiation time, and thickness of the semiconductor thin film. The J_{sc} for the cell increased with increasing thickness of semiconductor thin-film while the V_{oc} decreased due to increasing loss of injected electrons and the rate constant for the reverse reaction. Good stability of J_{sc} and V_{oc} was observed for over 24 h even when using an open cell. The turnover number per

mercurochrome molecule reached more than 18000 at least, indicating a sufficient stability of mercurochrome in this system under irradiation. These results showed the possibility of high performance of dye-sensitized solar cells using organic dyes as well as Ru complexes.

References

[1] B. O'Regan, M. Grätzel, Nature 353 (1991) 737.
[2] M.K. Nazeeruddin, A. Kay, I. Rodicio, R. Humphry-Baker, E. Muller, P. Liska, N. Vlachopoulos, M. Grätzel, J. Am. Chem. Soc. 115 (1993) 6382.
[3] H. Sugihara, L.P. Singh, K. Sayama, H. Arakawa, M. K. Nazeeruddin, M. Grätzel, Chem. Lett (1998) 1005.
[4] H. Gerischer, M.E. Michel-Beyerle, F. Rebentrost, H. Tributsch, Electrochim. Acta 13 (1968) 1509.
[5] H. Tributsch, H. Gerischer, Ber. Bunsen. Phys. Chem. 73 (1969) 251.
[6] H. Tsubomura, M. Matsumura, Y. Nomura, T. Amamiya, Nature 261 (1976) 402.
[7] N.J. Cherepy, G.P. Smestad, M. Grätzel, J.Z. Zhang, J. Phys. Chem. 101 (1997) 9342.
[8] S. Ferrere, A. Zaban, B.A, Gregg, J. Phys. Chem. 101 (1997) 4490.
[9] C. Nasr, D. Liu, S. Hotchandani, P.V. Kamat, J. Phys. Chem. 100 (1996) 11054.
[10] A.C. Khazraji, S. Hotchandani, S. Das, P.V. Kamat, PVJ. Phys. Chem. 103 (1999) 4693.
[11] K. Tennakone, A.R. Kumarasinghe, G.R.R.A. Kumara, K.G.U. Wijayantha, P.M. Sirimanne, J. Photochem. Photobiol. A 108 (1997) 193.
[12] K. Tennakone, G.R.R.A. Kumara, I.R.M. Kottegoda, V.P.S. Perera, P.S.R.S. Weerasundara, J. Photochem. Photobiol. A 117 (1998) 137.
[13] K. Sayama, M. Sugino, H. Sugihara, Y. Abe, H. Arakawa, Chem. Lett. (1998) 753.
[14] K. Gollnick, S. Held, J. Photochem. Photobiol. B 5 (1990) 85.
[15] K. Hara, T. Horiguchi, T. Kinoshita, K. Sayama, H. Sugihara, H. Arakawa, Chem. Lett. (2000) 316.
[16] B.W.P. Gomes, F. Cardon, Ber. Bunsen. Phys. Chem. 75 (1971) 194.
[17] K. Sayama, H. Sugihara, H. Arakawa, Chem. Mater. 10 (1998) 3825.
[18] K.K. Rohatgi, G.S. Singhal, J. Phys. Chem. 70 (1966) 1695.
[19] J. Moser, M. Grätzel, J. Am. Chem. Soc. 106 (1984) 6557.
[20] M. Hilgendorff, V. Sundström, Chem. Phys. Lett. 287 (1998) 709.
[21] K. Murakoshi, G. Kano, Y. Wada, S. Yanagida, H. Miyazaki, M. Matsumoto, S. Murasawa, J. Electroanal. Chem. 396 (1995) 27.
[22] R. Argazzi, C.A. Bignozzi, T.A. Heimer, F.N. Castellano, G.J. Meyer, Inorg. Chem. 33 (1994) 5741.
[23] K. Kalyanasundaram, M. Grätzel, Coord. Chem. Rev. 77 (1998) 347.
[24] D.E. Scaife, Solar Energy 25 (1980) 41.
[25] A. Hagfeldt, M. Grätzel, Chem. Rev. 95 (1995) 49.
[26] H.P. Maruska, A. Ghosh, Solar Energy 20 (1978) 443.
[27] S. Anderson, E.C. Constable, M.P. Dare-Edwards, J.B. Goodenough, A. Hamnett, K.R. Seddon, R.D. Wright, Nature 280 (1979) 571.
[28] H. Rensmo, K. Keis, H. Lindstrom, S. Sodergren, A. Solbrand, A. Hagfeldt, S.-E. Lindquist, L.N. Wang, M. Muhammed, J. Phys. Chem. B 101 (1997) 2598.
[29] T.N. Rao, L. Bahadur, J. Electrochem. Soc. 144 (1997) 179.
[30] M. Matsumura, K. Mitsuda, N. Yoshizawa, H. Tsubomura, Bull. Chem. Soc. Jpn. 54 (1981) 692.
[31] Y. Nishimura, H. Sakuragi, K. Tokumaru, Denki Kagaku (Electrochemistry) 62 (1994) 183.
[32] G. Redmond, D. Fitzmaurice, M. Grätzel, Chem. Mater** 6 (1994) 686.
[33] S. Södergren, A. Hagfeldt, J. Olsson, S.-E. Lindquist, J. Phys. Chem. 98 (1994) 5552.
[34] D. Liu, P.V. Kamat, J. Phys. Chem. 97 (1993) 10769.
[35] O. Kohle, M. Grätzel, A.F. Meyer, T.B. Meyer, Adv. Mater. (1997) 904.